RESEARCH ARTICLE

Mode Competition of Low Voltage Backward Wave Oscillator near 500 GHz with Parallel Multi-Beam

Xiaoyan ZHAO[1], Jincheng HU[1], Haoran ZHANG[2], Sidou GUO[1], Yuming FENG[1], Lin TANG[1], Kaichun ZHANG[1], and Diwei LIU[1]

1. *THz Center, School of Electronic Science and Engineering, University of Electronic Science and Technology of China, Chengdu 610054, China*
2. *School of Computer Science, Southwest Petroleum University, Chengdu 610500, China*

Corresponding author: Kaichun ZHANG, Email: zh.kch@163.com

Abstract — A backward wave oscillator with parallel multiple beams and multi-pin slow-wave structure (SWS) operating at the frequency above 500 GHz is studied. Both the cold-cavity dispersion characteristics and CST Particle Studio simulation results reveal that there are obvious mode competition problems in this kind of terahertz source. Considering that the structure of the multi-pin SWS is similar to that of two-dimensional photonic crystals, we introduce the defects of photonic crystal with the property of filtering into the SWS to suppress high-order modes. Furthermore, a detailed study of the effect of suppressing higher-order modes is carried out in the process of changing location and arrangement pattern of the point defects. The stable, single-mode operation of the terahertz source is realized. The simulation results show that the ratio of the output peak power of the higher-order modes to that of the fundamental mode is less than 1.9%. Also, the source can provide the output peak power of 44.8 mW at the frequency of 502.2 GHz in the case of low beam voltage of 4.7 kV.

Keywords — Mode competition, Backward wave oscillator, Multi-pin slow-wave structure, Parallel multiple beams, Defects.

Citation — Xiaoyan ZHAO, Jincheng HU, Haoran ZHANG, *et al.*, "Mode Competition of Low Voltage Backward Wave Oscillator near 500 GHz with Parallel Multi-Beam," *Chinese Journal of Electronics*, vol. 33, no. 2, pp. 488–495, 2024. doi: 10.23919/cje.2022.00.003.

I. Introduction

The terahertz (THz) band is between millimeter wave and infrared light, which has not been fully recognized and utilized by human beings. The terahertz waves have the characteristics of strong penetrating power, wide bandwidth, low quantum energy and so on. Hence, terahertz technology is widely used in biological imaging, materials science, deep space exploration, broadband communications and other fields [1]–[4]. With the rapid development of terahertz technology, high-power terahertz radiation sources have become one of the research hotspots of terahertz science and technology.

Vacuum electronics is one of the important ways to develop THz radiation sources. In 2007, High Frequency Integrated Vacuum Electronics (HiFIVE) Program [5] was launched, which mainly studied 220 GHz traveling wave tubes with an output power of about 50 W by a current density of 750 A/cm^2 and a focusing magnetic field of 1.0 T. Then, THz Electronics (THzE) Program was launched in 2008 for the research of 0.65–1.0 THz folded waveguide traveling wave tube amplifiers. For an amplifier operating at 0.66 THz, the output power is tens of milliwatts when its current density is about 150 A/cm^2 and the focusing magnetic field is about 0.9 T [6]. In 2009, the European Union proposed the OPTHER plan [7] to develop compact and novel vacuum THz radiation sources with a central frequency of 0.987 THz using a carbon nanotube cold cathode required a current density of 795 A/cm^2 and a focusing magnetic field of 0.8 T. Also, some

scholars studied a traveling wave tube around 0.3 THz with a current density of about 187 A/cm^2 and a focusing magnetic field of about 0.8 T and the output power about 21 W [8]. However, due to the increase in frequency, the size of vacuum electron devices is getting smaller and smaller and the current density is becoming higher and higher, making its processing and assembly very difficult. In addition, most applications require terahertz sources to be sufficiently efficient, compact, portable and capable of providing high-power output signals.

Based on the method of vacuum electronics, we designed a backward wave oscillator (BWO) with parallel multi-beam based on a novel slow-wave structure (SWS) composed of multiple parallel grating pins inside a quasi-rectangular waveguide [9]. The parallel multi-electron beam [10], [11] can highly decrease the operating current and current density compared to a single beam. In this paper, we extend our previous research on parallel multi-beam terahertz radiation source based on multi-pin SWS. By analyzing the dispersion relation of the SWS, we find that the multi-beam with a certain voltage may interact with multiple modes, causing multi-mode oscillation, which will adversely affect the stable output of the signal [12]. Therefore, the phenomenon of the multi-mode competition and mechanism of suppressing high-order modes is studied. The Calabazas Creek Research, Inc. (CRC) has conducted many researches on the terahertz BWO with SWS of the squared columns, and they also noticed the phenomenon of mode competition in the device [13], but did not propose a reasonable method to suppress the mode competition. While in this paper, we achieve the goal of single-mode, stable operation of the terahertz source by selecting the appropriate beam current and introducing point defects into the multi-pin SWS. In Section II, the unit cell of the SWS is given, and the cold parameter behavior is investigated with three-dimensional (3D) electromagnetic simulations. In Section III, two methods are proposed to suppress high-order modes in BWO with parallel multi-beam.

II. Eigenmode Calculation

In order to achieve a significantly higher output power at high operating frequency, a parallel multi-beam backward amplifier at 340 GHz based on the multi-pin rectangular waveguide SWS was proposed in [9]. In this paper, we plan to study a backward oscillator operating at the frequency above 500 GHz based on this schematic of multi-pin SWS and parallel multi-beam. The views of 3-D structure and cross section of the unit cell of the multi-pin SWS are shown in Figure 1. The main structure parameters are listed as $h = 0.33$ mm, $w = 0.7$ mm, $d = 0.06$ mm, $a = 0.1$ mm, $b = 0.11$ mm, $c = 0.03$ mm, $t = 0.2$ mm.

The boundary conditions of the multi-pin rectangular waveguide SWS are very complicated, and it is difficult to derive the mathematical expression of the dispersion relation. Therefore, we used the CST Microwave
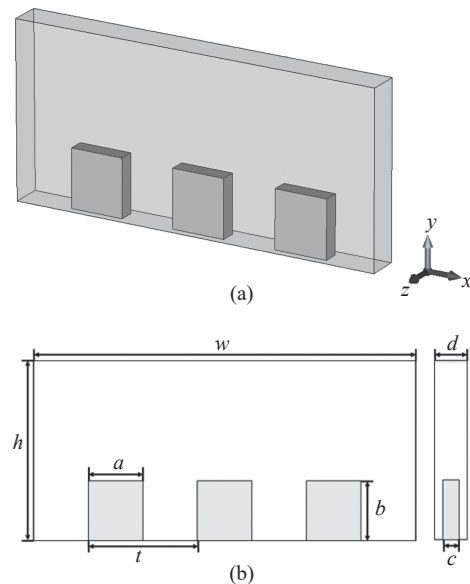

Figure 1 Unit cell of multi-pin rectangular waveguide SWS: (a) 3-D structure; (b) transverse and longitudinal cross section.

Studio [14] eigenmode simulations to extract the dispersion relation of the slow-wave structure. The results are shown in Figure 2, including the dispersion curves of TE$_{10}$-like, TE$_{20}$-like, and TE$_{30}$-like modes, as well as the dispersion curve of the 4.7 kV electron beam. The multi-pin SWS can be viewed as a derivative structure evolved from the corrugated rectangular waveguide SWS [15]–[17], the differences between them can be found in [11]. Compared with the latter, the dispersion curves of the former are closer to each other when the stopband is near the π point in the first Brillouin zone. From Figure 2, we can find that the intersection points between the beam and the modes are very close. This means that the beam probably interacts with the three modes and leads to multi-mode oscillation. When the electron beam with the energy of 4.7 keV, the intersection points of the beam line with the three modes are at the frequency of 530.5 GHz, 539.4 GHz and 542.6 GHz, respectively.

The Figures 3(a), (b) and (c) show the electric field distributions of the three models shown in Figure 2. It can be judged from the electric field vector distribution
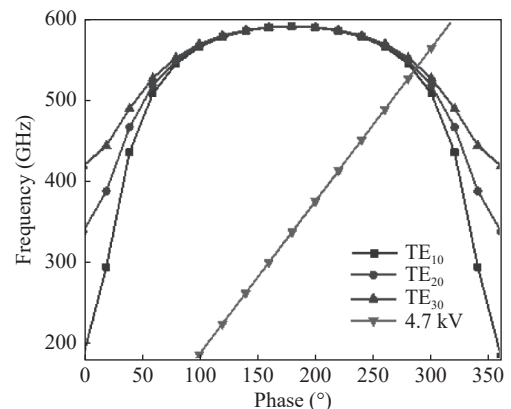

Figure 2 Dispersion characteristics of the multi-pin SWS.

diagrams that the three waves are respectively TE_{10}-like mode, TE_{20}-like mode and TE_{30}-like mode. The figures of electric field amplitude distribution show that the energy of TE_{10}-like mode is mainly confined to the second column of pins in the lateral direction, while TE_{20}-like mode is mostly concentrated on the first and third columns of pins in the transverse direction, and the amplitudes of the TE_{30}-like mode are approximately the same at the three horizontal rows of pins. Therefore, it can be inferred that the pins in the first and third column play a vital role in the propagation processes of high-order modes, but have little effect on the propagation of the fundamental mode. This provides the theoretical support for the next section to suppress the competitive modes by removing several pins in the first and third columns.
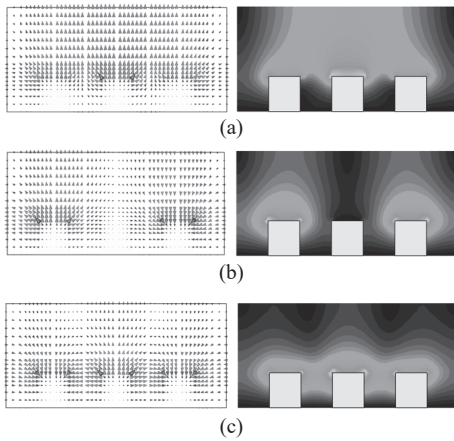

Figure 3 The electric field vector distributions (left) and the corresponding electric field amplitude distributions (right) of (a) TE_{10}-like mode, (b) TE_{20}-like mode, and (c) TE_{30}-like mode on the transverse cross section.

III. PIC Simulation

Based on the multi-pin SWS described above, a backward wave oscillator (BWO) with parallel multi-beam operating above 500 GHz and with the low voltage is designed and shown in Figure 4, which is simulated by CST Particle Studio [14]. The source is excited by 4 homogeneous cylindrical beams whose positions are shown in Figure 4(a), where $r = 0.04$ mm, $l = 0.08$ mm. The inset in Figure 4(b) shows the details of the 3-row pins SWS, in which the circuit is composed of 119-unit structures, including 7 transition structures at the rightmost and 7 transition structures at the leftmost. The material of pins is oxygen-free copper with default conductivity $\sigma = 5.88 \times 10^7$ S/m.

By PIC simulation, the beam voltage of the source is set as 4.7 kV. The power ratios of different modes are analyzed by means of Fourier method [18]. We find that the source can achieve single-mode output at the frequency of 502.2 GHz when the total current is low, such as in the range of 6–8 mA, but its output power is less than 5 mW to limit its practical application. In order to
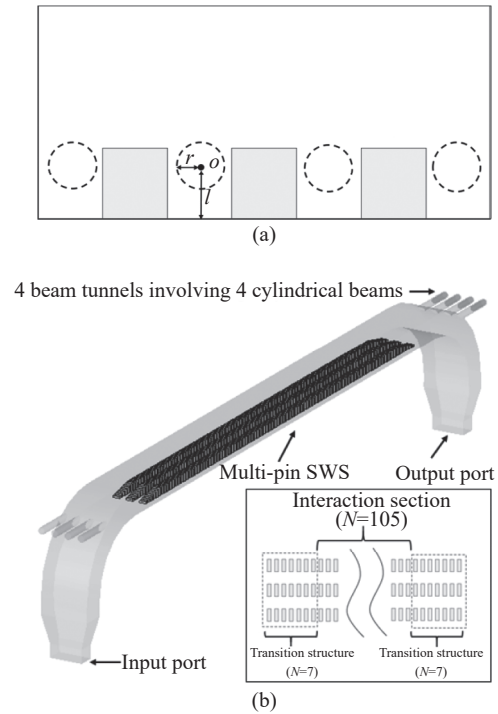

Figure 4 (a) Transverse section of multi-pin SWS; (b) Schematic diagrams of the 3-D structure of the BWO（(Inset) details of multi-pin SWS, where N is the number of longitudinal periods）.

obtain sufficient output power of the terahertz source, we increase the current up to 40 mA. Through simulation, it is found that the magnetic field should be increased with the increasing of the current, and that the magnetic field of 0.6 T has little effect on the performance of the BWO and can ensure 100% transmission of the electron beams when current is in the range of 6–40 mA. It is interesting that the output power can highly increase but the source cannot keep single-mode output. The result in Figure 5(a) shows the trend of the saturated output power of each mode versus the current. The output power gradually increases up to 125 mW when the current increases from 6 mA to 35 mA. However, increasing the beam current will lead to the problem of mode competition. And the corresponding mode competition relationship between the modes is shown in Figure 5(b). In this figure the two curves are the power ratio of TE_{20}-like mode to that of TE_{10}-like mode and the power ratio of TE_{30}-like mode to that of TE_{10}-like mode, respectively. We use the ratio to analyze the strength of the mode competition. When the total beam current is 35 mA, the strength of mode competition is less than 10%, but the corresponding current density is too large, which will make beam bunching so difficult and the volume of the focusing magnet so large that the source does not meet the requirements of portable, compact and lightweight terahertz sources for many applications. In addition, the mode competition is relatively strong when the total beam current is 25 mA, 30 mA and 40 mA. Therefore, in order to make the output power as large as possible and the mode competition intensity as small as possible, we

finally choose the beam current of 20 mA to study how to use pin defects to suppress the competitive modes of the BWO.
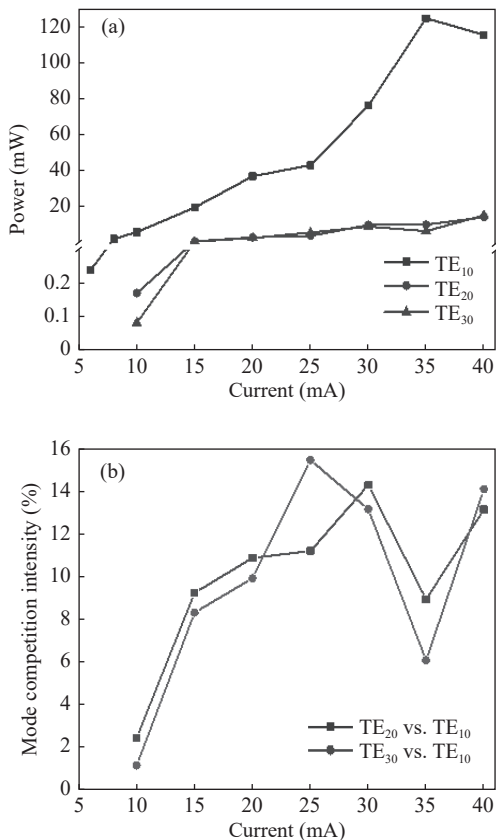

Figure 5 The output of terahertz source versus different beam currents when the voltage of 4 parallel-beam is 4.7 kV. (a) The relationship between output peak power and beam current; (b) The intensity of the mode competition between the higher-order modes and the fundamental mode.

When the voltage of the 4-beam is 4.7 kV, the current is 20 mA, and the focusing magnetic field is 0.6 T, the PIC simulation result of the signal voltage at the output port is shown in Figure 6. The output signal is not stable due to the multi-mode oscillation. By power spectrum analysis and band-pass filtering, we can observe that the amplitudes of three modes are very different. The oscillating frequencies of TE_{10}-like, TE_{20}-like and TE_{30}-like modes are 502.2 GHz, 514.3 GHz and 516.9 GHz, respectively.

In order to realize the single-mode operation with sufficient output power and avoid unnecessary parasitic modes excited by excessive beam current [19], [20], some methods should be taken to consider the suppression of the mode-competition. It is well known that the defect state of photonic crystal has the function of filtering and frequency selection [21]–[25]. The spatial structure of the multi-pin SWS is similar to that of the two-dimensional photonic crystal, so we consider removing the pins at specific positions of the slow-wave structure to suppress the competitive modes.
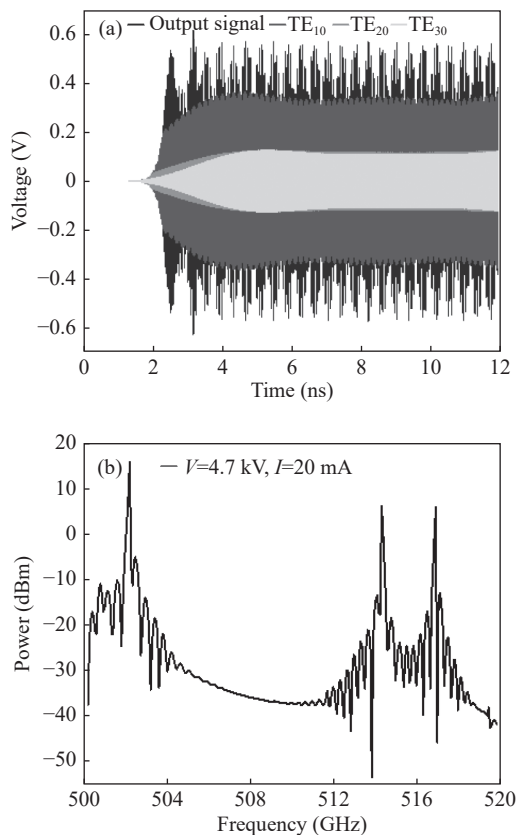

Figure 6 The output signal when 4-beam with the voltage of 4.7 kV and the total current of 20 mA: (a) the signal observed at output port; (b) power spectrum of the three modes.

In this paper, two types of point defect models are designed to achieve the optimum suppression effect by changing the position of the defects. Considering that the pins in the first and third columns dominate the propagation of TE_{20}-like mode and TE_{30}-like mode, we set the positions of the point defects in the first and third columns of the multi-pin array. Based on this, one pair of same-period point defects or the staggered point defects are set to analyze the mode suppression as shown in Figure 7.

When one pair of same-period point defects are set in the eighth period, the structural diagram of the SWS is shown in Figure 7(a). In order to obtain the signal closest to single-mode output, we change the position of defects and compare the suppression effect with point defects at different positions. When one pair of point defects are changed from the 8th period to the 112th period, the analytical results are shown in the Figure 8(a), where the normalized suppression effect of TE_{10}-like mode refers to the ratio of the output peak power of TE_{10}-like mode with defects to that of without defects, the normalized suppression effect of TE_{20}-like mode is the ratio of $(P_{outTE20}/P_{outTE10})$ with defects to that of without defects, and the normalized suppression effect of TE_{30}-like mode is similar to that of TE_{20}-like mode. As we can see from Figure 8(a), the output result is the best in the case that the pins in the first and third columns of the
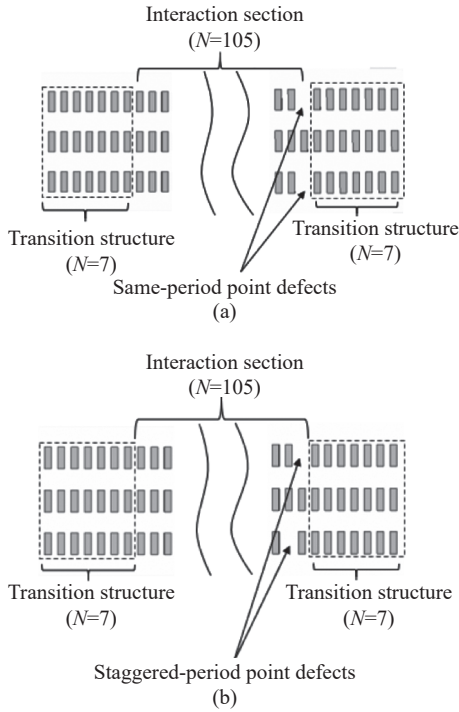
Figure 7 Defects schematic. (a) The same-period point defects; (b) The staggered-period point defects.

8th period are removed. In order to further clarify the best position of the defects, we move the defects from the 8th period to the 21st period, and the result is shown in Figure 8(b). Considering the output power of the fundamental mode and the suppression effect on the competition modes, we find that the effect is still the best when the pins in the first and third columns of the 8th period are removed. In this case the output signal and the filtering signal of the 3 modes are shown in Figure 8(c), and the power spectrum of the 3 modes is shown in Figure 8(d). By calculation, the ratio of the output peak power of the competition modes (TE_{20}-like mode and TE_{30}-like mode) to that of the fundamental mode is less than 2.6% and the corresponding fundamental mode output peak power is about 39.4 mW.

A simulation processing similar to that of same-period point defects is performed for the staggered point defects, and the results are shown in Figure 9. When staggered point defects are changed from the 8th period to the 112nd period with the change of 13-pin per step, it can be seen from the Figure 9(a) that the output signal is closest to the single-mode output signal when the defects in the first column of the 34th period and the third column of the 35th period are removed. Then we want to investigate the optimum suppression effect by adjusting the pin step near the staggered point defects of the 34th–35th period. So we move the defects from the 29th period to the 45th period with the change of 1-pin per step, and the results are shown in Figure 9(b). By comparison, we can find that the suppression effect is optimum when the staggered-period point defects are located in the first column of the 36th period and the third column of the 37th
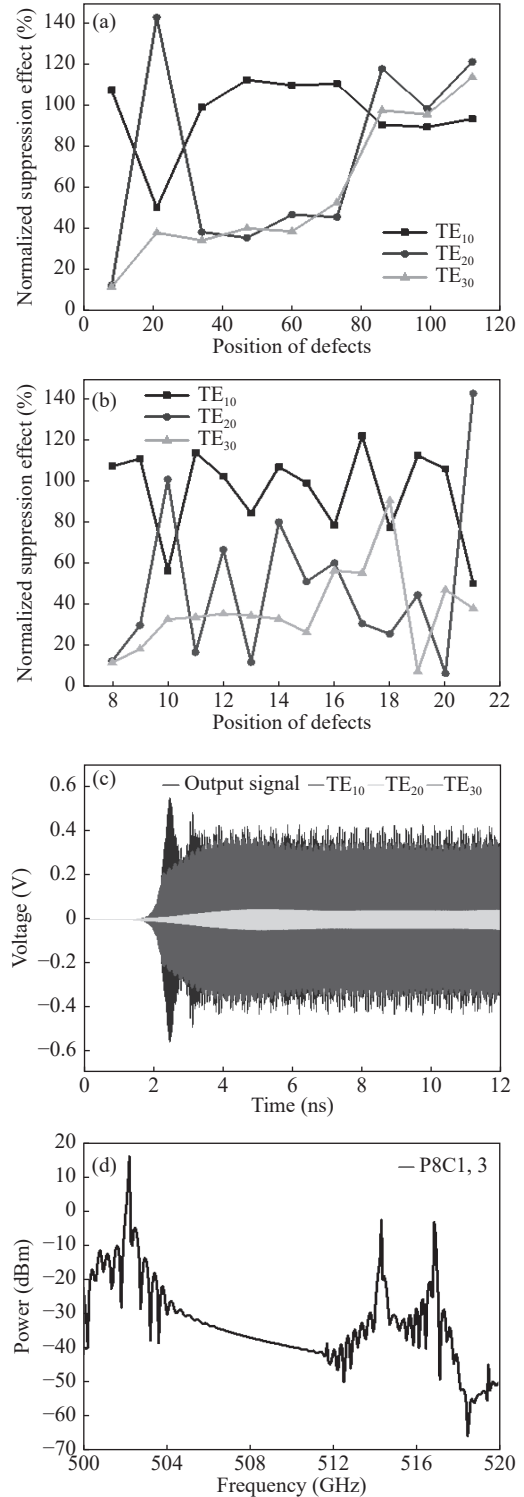

Figure 8 Influence of the point defects at different positions on the suppression effect. (a) The suppression effect of the same-period point defects on the competitive modes, when the point defect are in the 8th, 21st, 34th, 47th, 60th, 73rd, 86th, 99th, and 112nd periods; (b) The suppression effect of the same-period point defects located in the 8th to 21st in sequence; (c) Filter diagram of output signal when the same-period point defects located in the 8th period; (d) Power spectrum when the same-period point defects located in the 8th period.

period. In this case the fundamental mode output peak power is about 46.7 mW, and the output peak power ra-
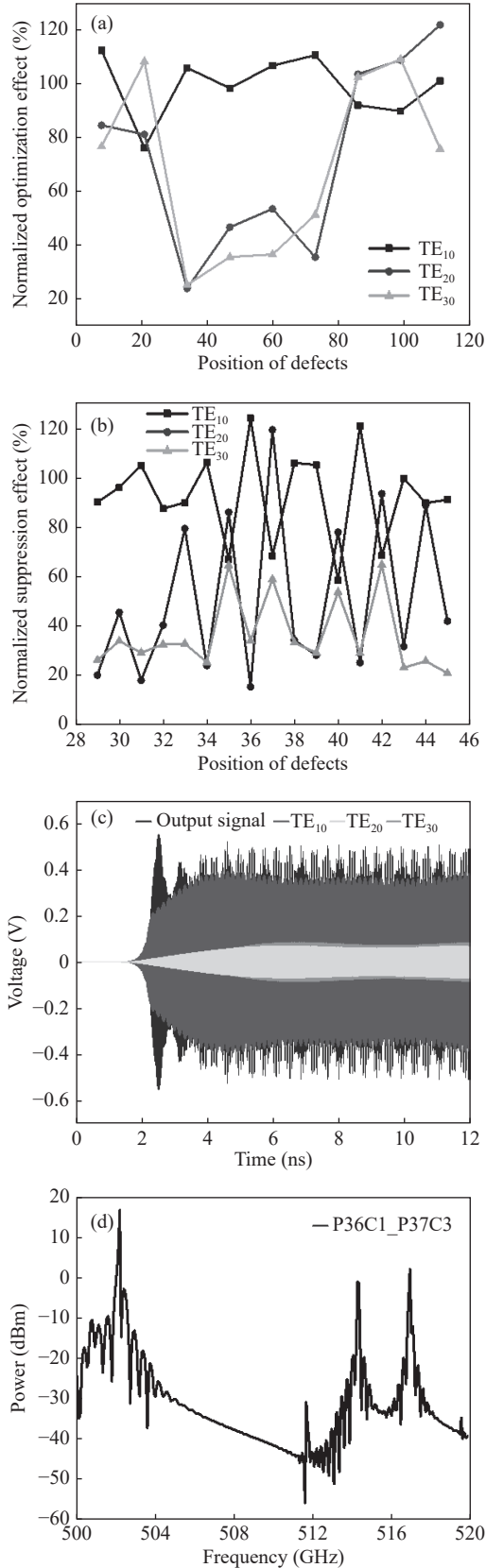
Figure 9 Same plots as in Figure 8 for the staggered point defects.

tio of the competitive modes (TE$_{20}$-like mode and TE$_{30}$-like mode) to the fundamental mode is about 5.0%.

Although the two types of defect states mentioned

above suppress the competition modes to a certain extent, we can still see two small resonance peaks from the power diagram in Figure 8(d) and Figure 9(d). Therefore, we combine the two types of defect states and obtain the output signal with the power of TE$_{10}$-like mode is about 44.6 mW at 502.2 GHz shown in Figure 10. Through analysis, we find that the ratio of the output peak power of the competitive modes to that of fundamental mode is about 1.9%, which is significantly better than the results when the two types of defect models are applied to the multi-pin SWS individually. In this case we can approximately obtain a single-mode output.
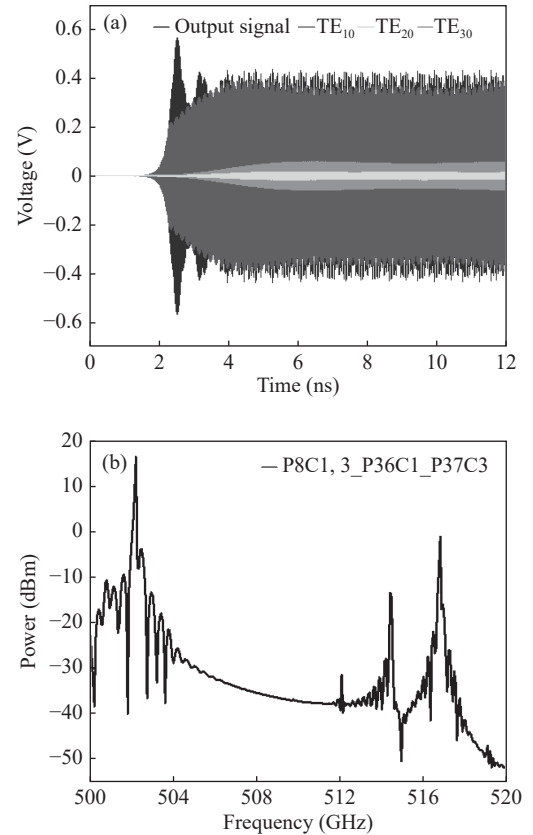

Figure 10 The output effect when combining the same-period point defects and staggered-period point defects at the optimal positions: (a) the output signal; (b) power spectrum when the first column and the third column of the 8th period are removed, as well as the pins of the first column of the 36th period and the third column of the 37th period.

IV. Conclusions

In this paper, the study on the mode competition of low voltage backward wave oscillator near 500 GHz with parallel multi-beam is carried out to achieve stable, single-mode operation of the terahertz source. Both the dispersion relation and the eigenmode field distributions of the SWS have been studied. The result indicates the existence of mode competition. By PIC simulation of a BWO, it is confirmed that the mode competition does exist under the condition of the beam voltage of 4.7 kV

and the current of 10–40 mA for 4 parallel beams. Due to the structural similarity between the multi-pin SWS and the two-dimensional photonic crystal, we propose the defects of the multi-pin SWS for the frequency selection and filtering. Two types of point defect models are designed for the SWS, the same-period defects model and the staggered point defects model. The former works best when the pins in the first and the third columns of the 8th period are removed, and the latter works best when the pins in the first column of the 41st period and the third column of the 42nd period are removed. Considering the output power and suppression effect comprehensively, we eventually combine these two kinds of point defect models and obtain the optimal output result. The simulation results show that the defect state of the multi-pin SWS is an effective method to suppress the mode competition of the BWO with parallel multi-beam. A miniature BWO with 44.8 mW single-mode output at 502.2 GHz is obtained for potential applications when the beam voltage is 4.7 kV and the total beam current of 4 parallel beams is 20 mA. Compared with the same type of terahertz source, the terahertz source designed in this paper has a lower voltage and current density in the same frequency band. For example, the voltage and current density of the terahertz source designed in this article is less than half of the rectangular corrugated waveguide terahertz source mentioned in [9], but the output power of the former far exceeds one-half of the power of the latter. This greatly reduces the requirements of the device for voltage source and bunching magnetic field, making the volume of magnet and device smaller. As a consequence, this lightweight, compact and portable source can provide high power with low voltage and low current for THz application in many areas.

This paper mainly focuses on the simulation design, theory and phenomenon analysis of the backward wave tube. The manufacturing and experimental verification of the model will be carried out in the next stage. At that time, issues such as material selection, machining technology, machining accuracy [26], and performance differences between simulation and reality [27], [28] will be fully discussed.

Acknowledgement

References

[1] P. H. Siegel, "Terahertz technology," *IEEE Transactions on Microwave Theory and Techniques*, vol. 50, no. 3, pp. 910–928, 2002.

[2] L. F. Gao, Y. M. Wang, Y. L. Hu, *et al.*, "Study of multiple beam backward wave oscillator based on corrugated waveguide TWT," in *Proceedings of the 2017 Eighteenth International Vacuum Electronics Conference*, London, UK, pp.1–2, 2017.

[3] J. F. Federici, B. Schulkin, F. Huang, *et al.*, "THz imaging and sensing for security applications—explosives, weapons and drugs," *Semiconductor Science and Technology*, vol. 20, no. 7, pp. S266–S280, 2005.

[4] M. Tonouchi, "Cutting-edge terahertz technology," *Nature Photonics*, vol. 1, no. 2, pp. 97–105, 2007.

[5] M. Basten, J. Tucek, D. Gallagher, *et al.*, "A multiple electron beam array for a 220 GHz amplifier," in *Proceedings of 2009 IEEE International Vacuum Electronics Conference*, Rome, Italy, pp.110–111, 2009.

[6] J. C. Tucek, M. A. Basten, D. A. Gallagher, *et al.*, "A 100 mW, 0.670 THz power module," in *Proceedings of IVEC 2012*, Monterey, CA, USA, pp.31–32, 2012.

[7] A. di Carlo, C. Paoloni, F. Brunetti, *et al.*, "The European project OPTHER for the development of a THz tube amplifier," in *Proceedings of 2009 IEEE International Vacuum Electronics Conference*, Rome, Italy, pp.100–101, 2009.

[8] X. B. Shi, W. H. Xiong, and C. H. Wen, "A 340GHz 20W staggered double vane traveling wave tube," in *Proceedings of 2019 International Vacuum Electronics Conference*, Busan, Korea (South), pp.1–2, 2019.

[9] K. C. Zhang, Z. K. Qi, and Z. L. Yang, "A novel multi-pin rectangular waveguide slow-wave structure based backward wave amplifier at 340 GHz," *Chinese Physics B*, vol. 24, no. 7, article no. 079402, 2015.

[10] G. X. Shu, C. Q. Zhou, H. Xiong, *et al.*, "Study of a high-order mode terahertz backward wave ocsillator driven by multiple sheet electron beams," in *Proceedings of the 2018 11th UK-Europe-China Workshop on Millimeter Waves and Terahertz Technologies*, Hangzhou, China, pp.1–2, 2018.

[11] K. C. Zhang, Q. Xu, N. Xiong, *et al.*, "Parallel multi-beam and its application in THz band," in *Proceedings of 2019 International Vacuum Electronics Conference*, Busan, Korea (South), pp.1–2, 2019.

[12] K. E. Kreischer, R. J. Temkin, H. R. Fetterman, *et al.*, "Multimode oscillation and mode competition in high-frequency gyrotrons," *IEEE Transactions on Microwave Theory and Techniques*, vol. 32, no. 5, pp. 481–490, 1984.

[13] R. L. Ives, C. Kory, M. Read, *et al.*, "Development of backward-wave oscillators for terahertz applications," in *Proceedings of SPIE 5070, Terahertz for Military and Security Applications*, Orlando, FL, USA, pp.71–82, 2003.

[14] C. Inc, *CST Studio Suite*, 2015.

[15] M. Mineo and C. Paoloni, "Double-corrugated rectangular waveguide slow-wave structure for terahertz vacuum devices," *IEEE Transactions on Electron Devices*, vol. 57, no. 11, pp. 3169–3175, 2010.

[16] B. D. McVey, M. A. Basten, J. H. Booske, *et al.*, "Analysis of rectangular waveguide-gratings for amplifier applications," *IEEE Transactions on Microwave Theory and Techniques*, vol. 42, no. 6, pp. 995–1003, 1994.

[17] C. Paoloni and M. Mineo, "Double corrugated waveguide for G-band traveling wave tubes," *IEEE Transactions on Electron Devices*, vol. 61, no. 12, pp. 4259–4263, 2014.

[18] X. Z. Li, J. G. Wang, R. Z. Xiao, *et al.*, "Analysis of electromagnetic modes excited in overmoded structure terahertz source," *Physics of Plasmas*, vol. 20, no. 8, article no. 083105, 2013.

[19] S. H. Kao, C. C. Chiu, K. F. Pao, *et al.*, "Fundamental and harmonic mode competition in the gyromonotron," in *Proceedings of the 2010 8th International Vacuum Electron Sources Conference and Nanocarbon*, Nanjing, China, pp.91−92, 2010.

[20] K. F. Pao, T. H. Chang, C. T. Fan, *et al.*, "Dynamics of mode competition in the gyrotron backward-wave oscillator," *Physical Review Letters*, vol. 95, no. 18, article no. 185101, 2005.

[21] F. L. Lin, G. X. Qiu, and Y. P. Li, "Characteristic analysis of a two-dimensional photonic crystal and its application in microcavity," in *Proceedings of SPIE 4918, Materials, Devices, and Systems for Display and Lighting*, Shanghai, China, pp.352–361, 2002.

[22] S. Y. Yan, F. G. Wu, X. Zhang, *et al.*, "Method of tuning frequency of the defect mode in two-dimensional square photonic crystals," *Modern Physics Letters B*, vol. 27, no. 8, article no. 1350054, 2013.

[23] S. Yamada, Y. Watanabe, Y. Katayama, *et al.*, "Simulation of light propagation in two-dimensional photonic crystals with a point defect by a high-accuracy finite-difference time-domain method," *Journal of Applied Physics*, vol. 92, no. 3, pp. 1181–1184, 2002.

[24] F. Gadot, A. de Lustrac, J. M. Lourtioz, *et al.*, "High-transmission defect modes in two-dimensional metallic photonic crystals," *Journal of Applied Physics*, vol. 85, no. 12, pp. 8499–8501, 1999.

[25] A. Sugitatsu, T. Asano, and S. Noda, "Line-defect–waveguide laser integrated with a point defect in a two-dimensional photonic crystal slab," *Applied Physics Letters*, vol. 86, no. 17, article no. 171106, 2005.

[26] S. Li, J. G. Wang, G. Q. Wang, *et al.*, "Theoretical studies on stability and feasibility of 0.34 THz EIK," *Physics of Plasmas*, vol. 24, no. 5, article no. 053107, 2017.

[27] X. Z. Li, J. G. Wang, J. Sun, *et al.*, "Experimental study on a high-power subterahertz source generated by an overmoded surface wave oscillator with fast startup," *IEEE Transactions on Electron Devices*, vol. 60, no. 9, pp. 2931–2935, 2013.

[28] J. G. Wang, G. Q. Wang, D. Y. Wang, *et al.*, "A megawatt-level surface wave oscillator in Y-band with large oversized structure driven by annular relativistic electron beam," *Scientific Reports*, vol. 8, no. 1, article no. 6978, 2018.

Xiaoyan ZHAO received the B.E. degree in School of Physics from University of Electronic Science and Technology of China (UESTC). She is currently studying for the M.S. degree in electronic science and technology in the School of Electronic Science and Engineering at University of Electronic Science and Technology of China, mainly engaged in the basic frontier and applied research of terahertz.

(Email: 1374889019@qq.com)

Kaichun ZHANG received the B.S. and M.S. degrees in Sichuan and Ph.D. degree in University of Electronic Science and Technology of China. His research interests inlude terahertz science and technology and its application. (Email: zh.kch@163.com)